

## Viscosity-dependent Fluorescence and Low-temperature Photochemistry of Mesoionic 4-Phenyl-1,3,2-oxathiazolium-5-olate

Niels Harrit\* and Arne Holm

Department of General and Organic Chemistry, University of Copenhagen, The H. C. Ørsted Institute, Universitetsparken 5, DK-2100 Copenhagen, Denmark

Ian R. Dunkin

Department of Pure and Applied Chemistry, University of Strathclyde, Cathedral Street, Glasgow G1 1XL

Martyn Poliakoff and James J. Turner

Department of Chemistry, University of Nottingham, Nottingham NG7 2RD, England

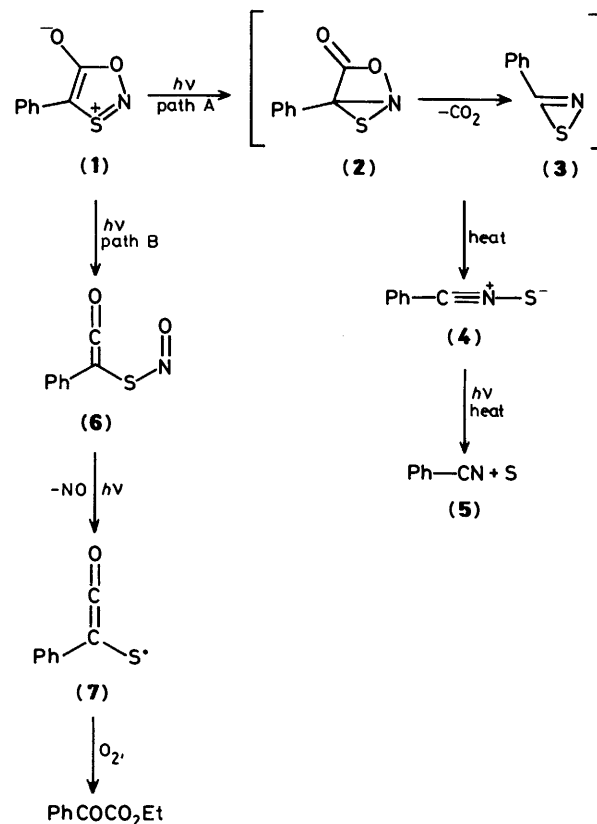
Irradiation of 4-phenyl-1,3,2-oxathiazolium-5-olate (**1**) at cryogenic temperatures leads to formation of benzonitrile sulphide (**4**) and phenyl(nitrosothio)ketene (**6**) as primary products. They have been characterized by u.v. and i.r. spectroscopy. The relative yields of (**4**) and (**6**) depend strongly on the local viscosity of the medium. For example, poly(vinyl chloride) favours the formation of (**4**), whereas solid nitrogen favours (**6**). The observation of a strong fluorescence is also conditioned by a rigid environment. A vibrational fine structure extending half way through the main absorption band of (**1**) indicates the existence of a dissociative pathway in the excited singlet-state potential energy surface. This pathway is identified with the formation of (**6**). Isotopic labelling has been used to characterize (**6**) and the i.r. absorptions of its *cis-trans*-isomers have been located. The *cis*-isomer of (**6**) can regenerate (**1**) upon irradiation; similar treatment of the *trans*-isomer leads to the resonance-stabilized radical phenyl(oxomethylene)thiyl (**7**).

When molecules are incorporated into a rigid medium strong restrictions are imposed on their translation, rotation, and nuclear rearrangement. Phenomena related to change in microscopic viscosity of the medium are more frequently recognized in photochemical than in thermal systems simply because thermal reactions are inhibited when viscosity rises. Except for the classical and thoroughly investigated *cis-trans* isomerization of stilbenes, the literature is devoid of reports on systems where viscosity-dependent emission and photochemistry can be correlated and understood. The photoinduced processes of 4-phenyl-1,3,2-oxathiazolium-5-olate (**1**) at low temperature have this potential<sup>1</sup> and are the subject of this paper.

Since phosphorescence spectra are routinely recorded in rigid glasses, the effect of viscosity<sup>2</sup> is rarely noticed. On the other hand, viscosity-dependent fluorescence yields have been widely observed and several classes of compounds have been investigated more or less thoroughly, e.g. the triphenylmethane dyes,<sup>3</sup> the stilbenes,<sup>4</sup> benzyliideneanilines,<sup>5</sup> dianthrones,<sup>6</sup> *trans*-1,1,4,4-tetraphenyl-2-methylbutadiene,<sup>7</sup> 1,2-di-(9-anthryl)ethylenes,<sup>8</sup> *p*-(dimethylamino)benzylidenemalononitrile,<sup>9</sup> and others.<sup>10</sup>

The photoinduced but thermally reversible transformation of nitrones into oxaziridines has been found to be influenced by the rigidity of polymer matrices.<sup>11</sup> Some 9-acylanthracenes fluoresce only in viscous media<sup>12</sup> and their photochemistry changes concomitantly.<sup>13</sup> It has therefore been concluded that rotation of the exocyclic acyl group must be an important deactivation mode of the excited singlet state in these aromatic ketones.

It is a common rule of thumb to disregard internal conversion from a high-energy first excited singlet state in approximations of kinetic expressions. Therefore, it is a striking feature common to all the reports on viscosity-dependent fluorescence enumerated here that they focus on internal conversion whenever the bottle-neck has to be found. The conformational changes sensitive to the rigidity of the environment and critical to internal conversion seem either to be of the free-rotor type (e.g. phenyl torsion) or torsion and out-of-plane bending of (dis)located double bonds.



Scheme 1.

As indicated in Scheme 1, 4-phenyl-1,3,2-oxathiazolium-5-olate (**1**) belongs to the class of heterocycles called mesoions. The photochemistry of (**1**) at room temperature<sup>14-16</sup> and at low temperature<sup>1,17,18</sup> has been described previously. The most commonly met photoreaction among mesoions is elimination of

a heterocumulene (*in casu* carbon dioxide) with simultaneous production of a (1,3)-dipole. In the case of (1) this path is labelled A and leads to benzonitrile (5). Path A may<sup>14</sup> start with formation of the bicyclic system (2) [a structure which can be considered as a valence tautomer of (1) and is identical with the formula originally suggested for the sydnones<sup>19</sup>] and proceed by elimination of carbon dioxide and generation of phenylthiazirine (3), a so-called anti-aromatic 4 $\pi$ -system. Benzonitrile sulphide (4) is produced from (3) by breaking the C-S bond. The final step leading to benzonitrile is extrusion of atomic sulphur.

The intermediacy of benzonitrile sulphide has been established firmly by trapping experiments<sup>14</sup> and by u.v. spectroscopy.<sup>17,18</sup> Structures (2) and (3) are still hypothetical intermediates in the photochemistry of mesoions. Strong evidence for a phenylthiazirine as a primary product and precursor for benzonitrile sulphide in the photochemistry of 5-phenyl-1,2,3,4-thiaziazoles has been established<sup>18</sup> in experiments performed at 10–15 K in poly(vinyl chloride) (PVC) matrices. After photolysis of (1) under the same conditions, a substantial re-formation of starting material, after heating to room temperature, was observed. It left an open question whether this is due to reaction between thiazirine and carbon dioxide or reflects the back-reaction from ketene (6) to (1) (see before and ref. 18). The work presented in this paper will support the last-mentioned mechanism.

Since their introduction by Piek,<sup>20</sup> the intermediacy of structures like (2) and (3) has been generally accepted throughout the reported photochemistry of mesoions (*e.g.* sydnones<sup>21,22</sup>). Kato *et al.*<sup>23</sup> have claimed that this type of sequence is general for the decomposition of mesoionic compounds. Gotthardt *et al.*<sup>16</sup> point out that formation of (2) from (1) is allowed as a disrotatory ring closure according to the rules for conservation of orbital symmetry. They also suggest that (2) could be a common precursor for (3) and (6). The fact is that the existence of both types of intermediate in the photochemistry of mesoions still remains to be proven.

Path B in Scheme 1 represents the alternative photochemical reaction mode for mesoions, *i.e.* ring opening. In the case of (1) and other systems<sup>24</sup> it competes with elimination. This step can be reversible so the fate of the heterocumulene (6) formed depends on several experimental parameters.<sup>15</sup>

Eber *et al.*<sup>22</sup> have found that the quantum yield for fluorescence of sydnones increases when the temperature is lowered from room temperature to 77 K. Simultaneously, the rate of non-radiative decay of the singlet goes down. These authors believe that temperature is the ruling experimental parameter and suggest that intersystem crossing is the critical deactivation mode associated with an Arrhenius barrier. Evans,<sup>25</sup> however, plots the results of Eber together with his own measurements and shows that viscosity of the surrounding medium and not the temperature is the factor determining the fluorescence quantum yield.

## Experimental

Experimental procedures for photolysis and spectroscopy at liquid nitrogen and lower temperatures were identical with those described in ref. 26. Deviations occurred in the choice of reference compounds for quantum yield determinations for the total emission spectra. In this case benzil and *N*-ethyl-4-nitroaniline were used (excitation wavelengths 374 and 395 nm, respectively).<sup>27</sup> The single-photon-counting apparatus is described in ref. 28.

The synthesis of 4-phenyl-1,3,2-oxathiazolylum-5-[<sup>18</sup>O]olate was based on the procedures developed by Wiberg and Fox<sup>29</sup> and Gotthardt.<sup>14</sup> Mercapto(phenyl)acetic acid (100  $\mu$ l) was dissolved in H<sub>2</sub><sup>18</sup>O (30%, containing 0.3% H<sub>2</sub><sup>17</sup>O). A catalytic amount of conc. HCl was added and the solution was

maintained at 80 °C for 46 h. The solvent was removed over conc. H<sub>2</sub>SO<sub>4</sub>. The labelled acid was dissolved in CH<sub>2</sub>Cl<sub>2</sub>-Et<sub>2</sub>O (4:1; 500  $\mu$ l) and EtONO (dry; 35  $\mu$ l) was added at 0 °C, followed by conc. H<sub>2</sub>SO<sub>4</sub> (2  $\mu$ l). After 10 min *N,N'*-dicyclohexylcarbodi-imide (DCC) (151 mg) dissolved in CH<sub>2</sub>Cl<sub>2</sub> (500  $\mu$ l) was added and the mixture was left for 5 min at 0 °C. The solution was warmed to room temperature and *N,N'*-dicyclohexyl[<sup>18</sup>O]urea (60 mg) was removed by filtration. Evaporation of the filtrate and recrystallization (MeOH; 1.5 ml) of the residue gave (1) (49 mg, 87%). According to the mass spectrum of the product <sup>15</sup> labelling was exclusively (30%) in the exocyclic position. No <sup>18</sup>O was incorporated in the ring.\*

## Results

**Electronic Absorption Spectroscopy.**—The electronic absorption spectrum of (1) in diethyl ether-isopentane-ethanol (5:5:2) (EPA) at 85 K is depicted as trace (a) in Figure 1. The long-wavelength band at 411 nm ( $\epsilon$  8.0 10<sup>3</sup> l mol<sup>-1</sup> cm<sup>-1</sup>; 20 °C) is ascribed to a  $\pi, \pi^*$  transition of the mesoionic ring.<sup>14</sup> No alkyl-1,3,2-oxathiazolylum-5-olates have been prepared, but analogy can be made with the sydnones, of which (1) can be considered as an aza-thia-analogue. 3-Methylsydnone displays only one absorption in its electronic spectrum<sup>30</sup> while that of 3-phenylsydnone features a less structured profile with several bands. Thus, it is reasonable to think of the two bands in the absorption spectrum of (1) as associated with the phenyl group (255 nm) and the mesoionic ring, respectively.

Since the long-wavelength band is symmetrical, equation (1)<sup>31</sup> is expected to be valid for calculation of the radiative

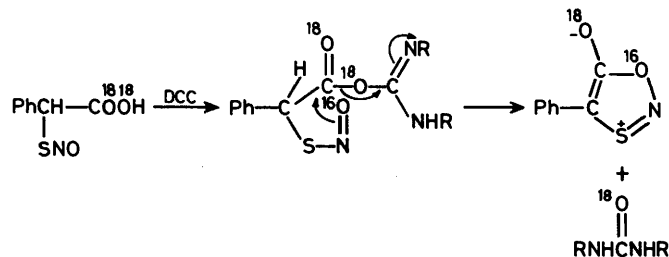
$$\tau_0 = \frac{3.5 \times 10^8}{\bar{\nu}_m^2 \epsilon_m \Delta \bar{\nu}_4} \quad (1)$$

lifetime of the first excited singlet state. Application leads to  $\tau_0$  (85 K) = 19 ns.

In EPA the absorption maxima are insensitive in shape and position to temperature changes in the range 85–300 K. A weak bathochromic effect has been observed in the room-temperature spectra of (1) in solvents of decreasing polarity.<sup>14</sup> However, in the non-polar isopentane-methylcyclohexane (1:1) (MPH) a dramatic hypsochromic shift is observed on cooling from 300 to 85 K (Figure 2). The maxima became flat and broad and the 415 nm transition is shifted to 380 nm. This process is reversible and most probably due to formation of dimers or aggregates at lower temperatures.

The absorption spectrum recorded at 10 K in an N<sub>2</sub> matrix reveals more details [Figure 12, trace (a)]. The 415 nm band has vibrational fine structure which starts on the long-wavelength side of the band but fades out and stops around 390 nm. The absence of fine structure in EPA is an expected consequence of the recognized heterogeneity among solvation sites in EPA.<sup>32</sup> In the N<sub>2</sub> matrix solvation energies are far smaller and the vibrational fine structure can be seen. The vibrational spacing increases gradually from 400 cm<sup>-1</sup> at 470 nm to 600 cm<sup>-1</sup> at 390

\* This observation agrees with the *a priori* expected reaction sequence:



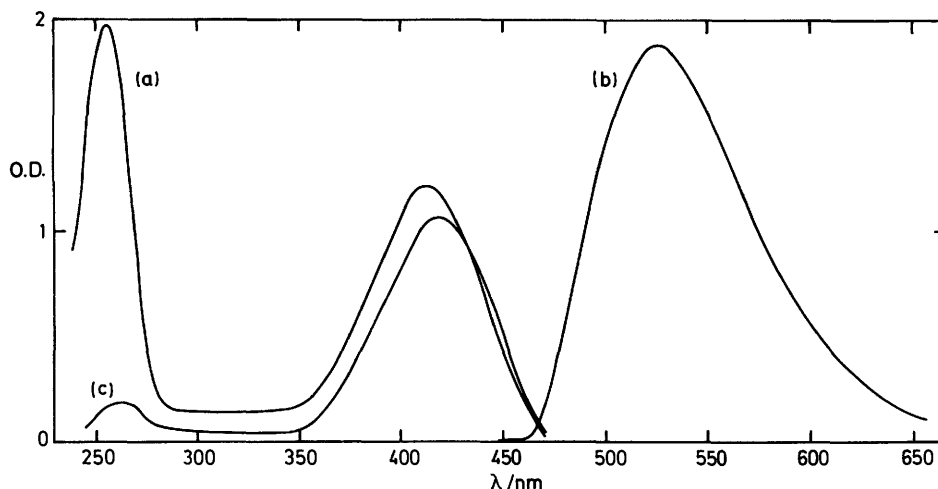


**Figure 1.** (a) Electronic absorption spectrum of (1) in EPA at 85 K; (b) uncorrected total emission spectrum of (1) in EPA at 77 K [intensity scale arbitrary; excitation wavelength 380 nm; concn.  $4.6 \times 10^{-4}$  M (at room temp.)]; (c) corrected excitation spectrum of (1) in EPA at 77 K [concn.  $7.5 \times 10^{-6}$  M (at room temp.); monitored at 523 nm; intensity normalized with absorption spectrum at 430 nm]

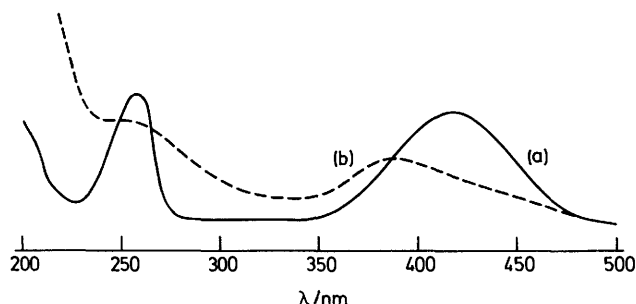


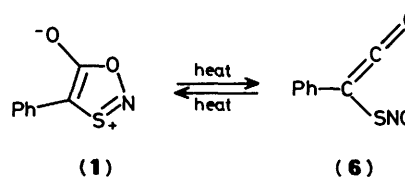
**Figure 2.** Electronic absorption spectrum of (1) in MPH: (a) room temperature; (b) 85 K. Cooling took *ca.* 2 h

nm. The short-wavelength maximum is split in an irregular manner into a shoulder at 248 nm, and two sharp peaks at 255 and 259 nm. The background (an impurity in the CsBr plate) represents a complication in this region but cannot be responsible for any of the observed absorptions since neither intensities nor the wavelength readings fit. The shoulder at 248 nm, however, is assigned to the presence of small amounts of phenyl(nitrosothio)ketene (6) (see later). Since the sample was prepared in absolute darkness by co-condensation of (1) and the matrix gas, the observation leads to the conclusion that an equilibrium between (1) and (6) exists in the gas phase (Scheme 2).

The splitting of the 255 nm absorption in two sharp peaks at 255 and 259 nm is attributed to two relaxed states of the phenyl group with respect to torsion. The difference in excitation energy amounts to  $778 \text{ cm}^{-1}$ .

**Emission.**—The mesoion (1) shows no emission in fluid solutions at room temperature. Neither is any long-lived emission (*e.g.* phosphorescence) to be seen at 77 K in EPA. However, by removing the rotating shutter from the emission spectrograph a very intense yellow emission ( $\lambda_{\text{max}}$ , 523 nm) could be observed under these circumstances [trace (b) Figure 1]. Almost identical emission spectra were recorded in a variety of plastics at 77 and 194 K and in glycerol at 194 K.\*

\* The following values for  $\lambda_{\text{max}}$ , nm have been obtained: EPA 523, poly(vinyl chloride) 524, poly(methyl methacrylate) 521, poly(vinyl acetate) 527, polystyrene 529, and glycerol (194 K only) 509 nm.



**Scheme 2.**

No emission could be observed from (1) embedded in solid  $\text{N}_2$  at 10 K or from the neat crystals at the same temperature.

The excitation spectrum [Figure 1, trace (c)] of the emitting molecule was recorded in EPA at 77 K and corrected manually according to the procedure of Parker<sup>33a</sup> with rhodamine B in ethylene glycol as quantum counter. In other systems, this set-up and procedure has led to coinciding absorption and excitation spectra. In the case of (1), however, a pronounced deviation is observed in the 255 nm region. An explanation for the weak maximum in the excitation spectrum may be that deactivation from this upper excited singlet  $\pi, \pi^*$  state of the phenyl group starts *ca.*  $184 \text{ kJ mol}^{-1}$  above the state(s) generated by excitation at 411 nm. The large energy gap makes deactivation modes other than internal conversion more competitive. Despite this quantitative discrepancy, the excitation spectrum points towards the monomer molecule of (1) as the emitting species since both absorption maxima are clearly located and the absorption spectrum in EPA [Figure 1, trace (a)] shows no sign of aggregation (compare Figure 2).

The lifetime of the emission in EPA at 77 K was determined by single-photon counting to be 8.5 ns. The quantum yield of the emission at 77 K in EPA was measured according to the procedure of Parker<sup>33a</sup> as  $\phi_{\text{em}}(\text{EPA}; 77 \text{ K}) = 0.13 \pm 0.02$ .

This leads to an experimental radiative lifetime ( $\tau_0$ ) of 65 ns, which identifies the emission as prompt fluorescence.

The quantum yield of fluorescence as a function of temperature was determined by recording the output during the warm-up of the glassy EPA solution from liquid nitrogen temperature. The resulting curve is displayed in Figure 3.

**Quenching Experiments at Room Temperature.**—Experiments in liquid solution at room temperature were performed in order to establish the multiplicity of the excited state involved in photolysis. The quantum yield for disappearance of (1) in a  $10^{-3}$  M solution in ethanol saturated with oxygen was deter-

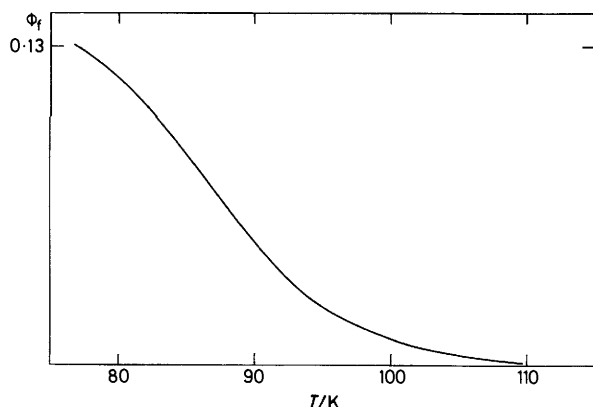


Figure 3. Quantum yield of emission as function of temperature in EPA (heating rate 8 K min<sup>-1</sup>; exc. wavel. 380 nm; concn. 1.0 × 10<sup>-4</sup>M)

mined by means of potassium ferrioxalate actinometry<sup>33c</sup> as  $\phi_f$  (370 nm; 20 °C; EtOH; O<sub>2</sub>) = 0.36 ± 0.04. Using a merry-go-round and freeze-pump-thaw cycles to remove oxygen, relative quantum yields in degassed and oxygen-saturated samples were determined. Photolysis turned out to be 20% slower in the absence of oxygen. No suitable sensitizers were found owing to the intense long-wavelength absorption of (1). Instead, both anthracene ( $E_T$  42 kcal mol<sup>-1</sup>)\* and piperylene (spectroscopic triplet 57 kcal mol<sup>-1</sup>) were investigated as quenchers. In both cases the samples were degassed. Within error, the presence of anthracene had no effect on the photolytic degradation of (1). In the samples with piperylene, a two-fold faster reaction was observed. In the last case, chromatographic analysis (t.l.c. and g.l.c.) indicated a reduced yield of benzonitrile as compared with the degassed samples, and the formation of polymers.

When a photochemical reaction is accelerated by the presence of oxygen, one is tempted to suggest that singlet molecular oxygen is involved. It can be formed by quenching of excited substrate triplets and may then react with ground-state molecules, thus accelerating the rate of photodestruction. As shown earlier, this is not the case.<sup>15</sup> Triplet (1) is formed and is quenched but the enhanced quantum yield is due to chemical trapping of either (6) or (7).<sup>15</sup> The action of piperylene is probably of the same kind. For example, (7) can induce a radical-chain reaction among the diene molecules. Oxygen as well as anthracene and piperylene are considered efficient quenchers, deactivating triplets more efficiently than singlets owing to the longer lifetime of the excited triplet state. When they all fail to retard the room-temperature photolysis, the photochemistry of (1) must follow a singlet pathway.

*Photolytic Transformations at Low Temperature.—EPA and MPH glasses; PVC film; 85 K; u.v. spectroscopy.* Preliminary accounts of the photochemistry of 4-phenyl-1,3,2-oxathiazolium-5-olate (1) at low temperature in EPA have been presented.<sup>1,17,18</sup> Irradiation produces the characteristic spectrum of benzonitrile sulphide (4) at 240s, 295, 313, 324, and 335 nm. The spectral transformation displays isosbestic points at 351 and 255 nm (Figure 4). The quality of these, however, depends on the initial concentration of (1). At concentrations higher than that used in Figure 4, deviations occurred. In Figure 5 the absorbance at 335 nm is plotted against the extinction at 411 nm. A straight line corresponds to the observation of isosbestic points. An upwards bend is seen to occur sooner with higher initial concentrations. This observation implies the

occurrence of secondary reactions leading to benzonitrile sulphide.

Upon heating of the sample, the spectrum remained unchanged until melting of the glass started around 140 K. Crystallization phenomena rendered spectral observations impossible during this process. Afterwards all the benzonitrile sulphide had disappeared and the characteristic absorptions of benzonitrile could be observed at 233 ( $\epsilon$  1.3 10<sup>4</sup> l mol<sup>-1</sup> cm<sup>-1</sup>),<sup>34</sup> and 271 nm in ca. 70% yield based on (1). Benzonitrile was also formed photolytically from benzonitrile sulphide when exposed to 335 nm light at 85 K instead of heating. Simultaneously small amounts (ca. 5%) of starting material were formed. Further indication of secondary (photo)processes became apparent from other experiments where the exciting wavelength was changed to 370 nm after exhaustive irradiation at 420 nm [Figure 6, trace (b)]. This caused a striking 50% increase in the amount of benzonitrile sulphide formed [Figure 6, trace (c)] despite the fact that ca. 90% conversion of (1) had taken place prior to continued irradiation. From the experiment depicted in Figure 6, a lower value (assuming 100% conversion) for the extinction coefficient of benzonitrile sulphide at 335 nm could be determined:  $\epsilon(4)_{355} = 6.7 \times 10^3$  l mol<sup>-1</sup> cm<sup>-1</sup>.

Photolysis of (1) in a PVC film at 85 K proceeded quantitatively the same way as in EPA. On irradiation (400 ± 14 nm) benzonitrile sulphide was formed with maxima at 337, 317br, sh, 293, and 242 nm. In comparison with that in EPA, the spectrum was smeared out: the maxima were less sharp, and the weak maximum at 324 nm could not be seen. Furthermore, some benzonitrile was formed along with benzonitrile sulphide even when irradiation was performed at 440 nm. The important feature of PVC as medium for photolytic conversions is its preserving effect on labile intermediates. While benzonitrile sulphide breaks down along with the melting of the EPA glass the thermal conversion into benzonitrile in PVC is gradual and traces of (4) could be detected even at room temperature. The profile of the decay can be very useful when correlation between experiments employing u.v. and i.r. spectroscopy is to be made.

Photolysis of (1) in MPH at 85 K followed by electronic absorption spectroscopy did not proceed any differently from the experiments in EPA and PVC. But, as expected, all spectral absorptions of the resulting benzonitrile sulphide were flat and broad like those displayed by the starting material in Figure 2. Also, the sensitivity of (1) towards light was strongly reduced in comparison with the EPA solutions. Since MPH does not tend to crystallize when thawing, the thermal conversion of benzonitrile sulphide into benzonitrile could be estimated to occur at ca. 140 K in that solvent.

Analogous results were obtained by photolysing 4-(4-bromophenyl)-1,3,2-oxathiazolium-5-olate in EPA at 85 K. The u.v. absorptions from 4-bromobenzonitrile sulphide were found at 251, 300, 321, 330, and 343 nm.

To confirm the yield of benzonitrile determined spectroscopically, a 10<sup>-2</sup>M-solution of (1) in neat ethanol was irradiated (390 nm) at 77 K. After melting, the yield of benzonitrile was determined (g.l.c.) to be 70%. Furthermore, the presence of nitroso thiols after melting was established by means of the specific test developed by Saville.<sup>15,35</sup>

*N<sub>2</sub> Matrix; 10 K; i.r. spectroscopy.* In agreement with its structural representation, the mesoion (1) has a considerable dipole moment (4.5 D).<sup>36</sup> This is reflected in its tendency to aggregate in media with low dispersing power like gas matrices. Preliminary attempts to sublime and co-condense (1) with nitrogen (or methane) on a CsBr window (20 K) followed by i.r. spectroscopy (10 K) revealed two carbonyl stretch frequencies at 1750 and 1710 cm<sup>-1</sup> [Figure 7, trace (a)]. Prolonged annealing (10–30 K) caused an increase in the 1710 cm<sup>-1</sup> band at the expense of the band at 1750 cm<sup>-1</sup>. Permitting the matrix

\* 1 kcal = 4.184 k J.

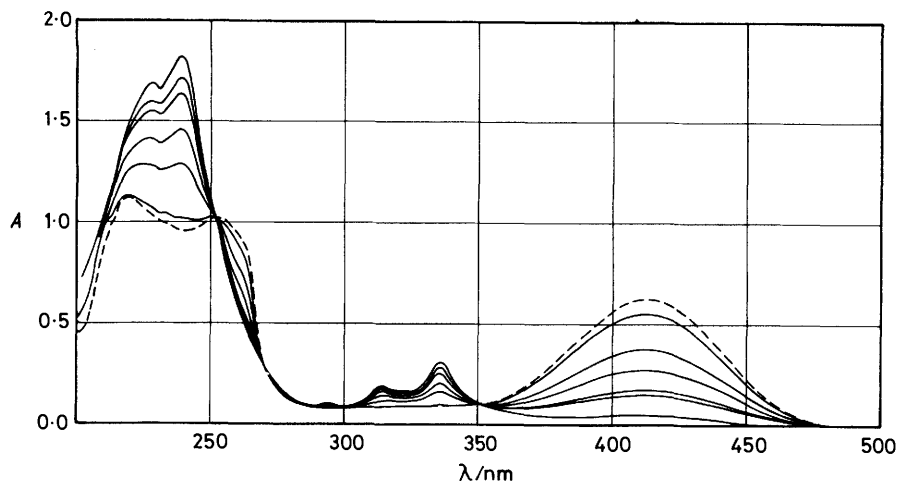


Figure 4. Photolyses of (1) ( $420 \pm 7$  nm) in EPA at 85 K (concn.  $5 \times 10^{-5}$  M); u.v. spectra recorded in intervals increasing from 3 to 30 min

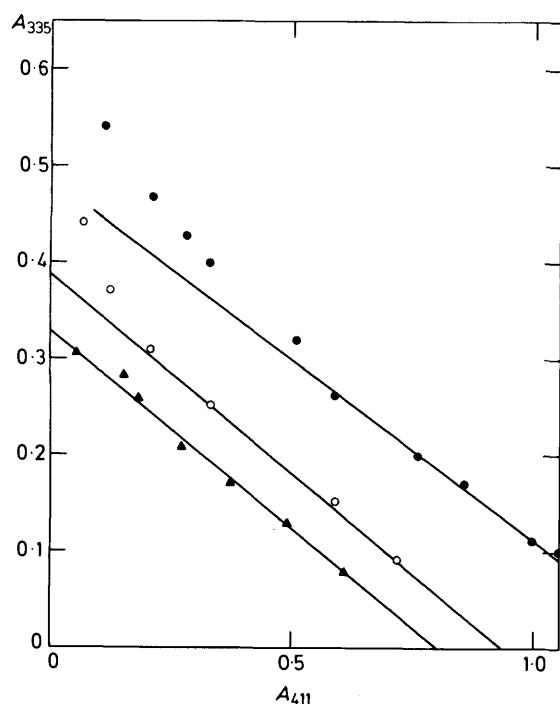


Figure 5. Absorbance at 335 nm as function of absorbance at 411 nm recorded during photolysis (420 nm) of (1) in EPA at 85 K. Three experiments with different initial concentrations are depicted. The curve closest to zero corresponds to Figure 4

gas to evaporate resulted in complete disappearance of the  $1750\text{ cm}^{-1}$  band [Figure 7, trace (b)]. This, therefore, is assigned to the isolated molecule of (1), while the  $1710\text{ cm}^{-1}$  band appears when the molecules aggregate.\* A similar shift is observed in the i.r. spectrum of (1) in tetrachloroethylene ( $1745\text{ cm}^{-1}$ ) as compared with a common KBr disc ( $1700$

\* The following absorptions ( $\text{cm}^{-1}$ ) are specific for the monomer form of (1):  $1750\text{vs}$  and  $1595\text{m}$ . The following absorptions are specific for the aggregated form:  $1710\text{vs}$ ,  $1187\text{w}$ ,  $1153\text{w}$ ,  $1078\text{w}$ ,  $1055\text{w}$ ,  $910\text{w}$ ,  $888\text{w}$ ,  $713\text{w}$ ,  $700\text{w}$ , and  $503\text{s}$ . The following absorptions are common to both forms:  $1495\text{w}$ ,  $1476\text{w}$ ,  $1446\text{w}$ ,  $1346\text{w}$ ,  $1335\text{w}$ ,  $958\text{m}$ ,  $875\text{s}$ ,  $760\text{s}$ ,  $685\text{w}$ ,  $680\text{s}$ ,  $665\text{w}$ ,  $595\text{m}$ , and  $513\text{m}$ .

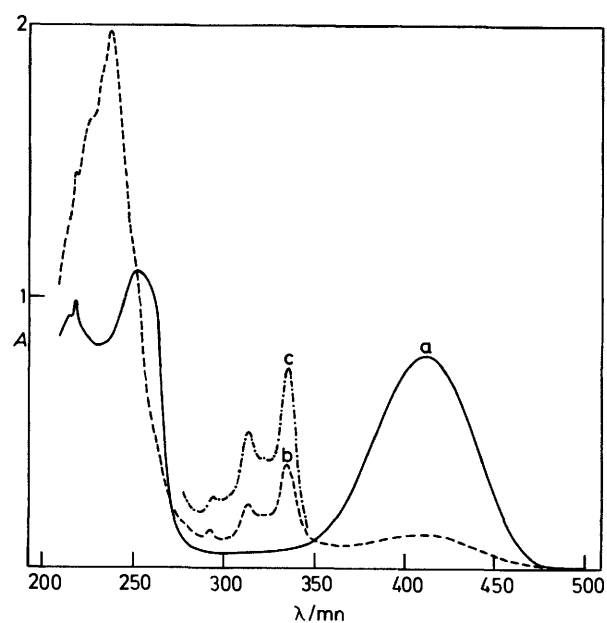


Figure 6. U.v. spectra of (1) in EPA (concn.  $1.0 \times 10^{-4}$  M) at 85 K: (a) before irradiation; (b) after irradiation for 110 min at  $415 \pm 7$  nm; (c) after further irradiation for 100 min at  $370 \pm 7$  nm

$\text{cm}^{-1}$ ).<sup>14</sup> As determined by X-rays,<sup>36</sup> the molecules of the parent mesoion are aligned head-to-tail in the crystal lattice. This observation agrees well with the shift in i.r. frequency of the C—O group observed when the isolated molecules of the gas matrix are permitted to aggregate. The dipole moment of the molecule parallels the C—O bond which is weakened when the charge separation is reduced by aggregation.

The isolated and aggregated forms of (1) in the  $\text{N}_2$  matrix showed strikingly different photochemical behaviour.<sup>1</sup> When both were present in the same sample, the isolated molecules reacted much faster than the aggregated. By slow and careful application, matrices free of aggregated guest molecules could be prepared. Figure 8 displays the i.r. spectrum recorded after photolysis of such a sample. The sensitivity was very high and the primary absorption of the product shoots up to  $2115\text{ cm}^{-1}$  [trace (a)]. Along with this band, absorptions appear at  $1594\text{m}$ ,  $1572\text{s}$ ,  $1500\text{m}$ ,  $1450\text{m}$ ,  $1200\text{w,br}$ ,  $753\text{m}$ , and  $692\text{m}$

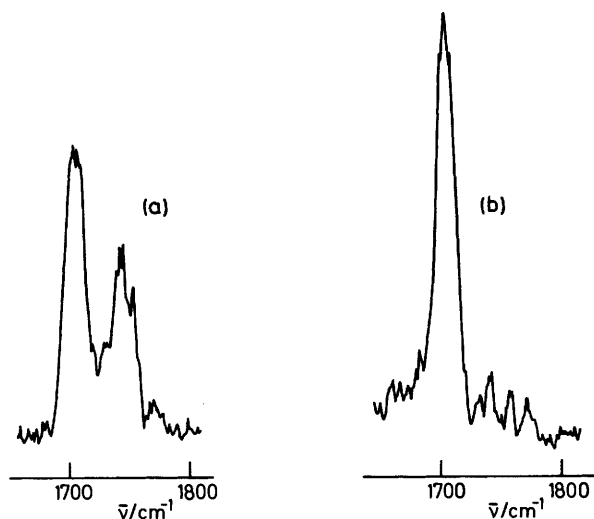


Figure 7. I.r. spectra (extinction upwards) of (1): (a)  $N_2$  matrix at 20 K; (b) same sample warmed to 200 K and re-cooled to 10 K

$cm^{-1}$ . The first two mentioned are the most important. The band at  $1572\text{ cm}^{-1}$  appeared immediately while that at  $1594\text{ cm}^{-1}$  seemed to be a result of prolonged irradiation. It does not therefore belong to the starting material, which displays a transition at almost the same frequency (see preceding footnote). All these absorptions are assigned to phenyl(nitrosothio)ketene (6).<sup>1</sup> Extended irradiation proved that (6) can undergo secondary photolysis. Figure 8, trace (c), represents a situation where all the starting material has been converted. The off-scale absorption of (6) is accompanied by a tiny peak at  $2055\text{ cm}^{-1}$ . This is due to the natural occurrence of centre- $^{13}C$ -substituted (6). Formation of carbon dioxide is observed at  $2340\text{ cm}^{-1}$ . Extended irradiation by the unshielded light from the Phillips HPK-125 lamp caused destruction of phenyl(nitrosothio)ketene and production of carbon dioxide together with new peaks at  $2040$  and  $2132\text{ cm}^{-1}$ . The first is assigned to phenyl(oxomethylene)thiyl (7), which is known to be formed along with NO in the room-temperature photolysis of (6) (Scheme 1). The shift towards lower frequency for the heterocumulene moiety of (7) as compared with (6) reflects a weakening of the cumulated double bond as described by the two resonance structures displayed in Scheme 5.

The absorption at  $2132\text{ cm}^{-1}$  is due to carbon monoxide.\* This is believed to be formed along with the thiobenzoyl radical in a photolytic destruction of (7) (Scheme 5). Alternatively, the carbon monoxide could originate from (6), which seems unlikely, since homolytic scission of the S-N bond of (6) is very efficient.<sup>15</sup> No absorptions assignable to the thiobenzoyl radical have been located. Furthermore, the presence of minor amounts of benzonitrile is betrayed by the small absorption at  $2220\text{ cm}^{-1}$ .

To facilitate the assignments, experiments were performed with (1) labelled in the exocyclic position by  $^{18}O$  (30% enriched in  $^{18}O$  with 0.3%  $^{17}O$ ). The carbonyl stretch frequency from [ $^{18}O$ ]- (1) in the isolated state was found at  $1726\text{ cm}^{-1}$ . The products observed after photolysis of such a sample free from aggregates are displayed in Figure 9. Besides  $2115\text{ cm}^{-1}$  (off-scale) new absorptions are seen at  $2085$  and  $2099\text{ cm}^{-1}$  (weak). They are due to the  $^{18}O$ - and  $^{17}O$ -substituted ketene, respectively. When these frequencies are compared with those of

\* CO Absorbs in Ar matrix at  $2138\text{ cm}^{-1}$  (associates) and  $2148\text{ cm}^{-1}$  (monomers).<sup>37</sup>

the corresponding methylketenes<sup>38</sup> (gas phase; room temperature) a satisfying correspondence is noted (Scheme 3). In particular, these numbers reflect the fact that most of the translational movement of the asymmetric vibration of ketenes is concentrated in the centre atom, which becomes most sensitive to isotopic substitution.

Importantly, the absorptions also assigned to phenyl(nitrosothio)ketene at  $1572$  and  $1594\text{ cm}^{-1}$  did not display any splitting as a consequence of the isotopic labelling. Therefore, these two bands are assigned to the N-O stretch vibration of the nitrosothiyl group of *cis*- and *trans*-(6), respectively (Scheme 5). This assignment is based on comparison with the nitrites, being the oxygen analogues of nitroso thiols. Nitrites feature a similar splitting in the gas phase<sup>39</sup> as well as in liquid<sup>40</sup> (Scheme 4).

So far, however, known spectra of *S*-nitroso thiols in the gas phase (*S*-nitrosoethanethiol,<sup>40,41</sup>  $1534\text{ cm}^{-1}$ ) and in solution (*S*-nitrosotriphenylmethanethiol,<sup>42</sup>  $1400$ – $1500\text{ cm}^{-1}$ ) show only one broad but unsplit band in this region. The absorptions displayed in Figure 8, trace (b), thus represent the first observation of *cis*-*trans* isomerism among nitroso thiols. This may be interpreted as a relatively large contribution of the canonical structure (6) (Scheme 4) to the electron distribution of (6), thus emphasizing the double-bond character of the S-N bond and the valence isomer relationship to the parent mesoion (1). This situation is also reflected in the fact that the absorption frequency of (6) falls in between those of alkyl nitroso thiols and nitrites.

*Crystal film; 10 K; i.r. spectroscopy.* The course of photolysis when the matrix gas was permitted to evaporate, leaving a thin crystal film behind, was quite different. In comparison with the monomeric sample, the crystal film reacted with much less efficiency. The spectrum of the products formed by photolysis of unlabelled (1) is displayed in Figure 10. Formation of the ketene (6) is seen to be greatly subdued, favouring elimination of carbon dioxide ( $2330\text{ cm}^{-1}$ ) to form benzonitrile ( $2220\text{ cm}^{-1}$ ).

A parallel experiment with  $^{18}O$ -labelled mesoion produced the absorptions displayed in Figure 10, trace (b). New peaks are located at  $2080\text{ cm}^{-1}$ , due to [ $^{18}O$ ]- (6), and  $2318\text{ cm}^{-1}$ , due to  $^{18}O=^{12}C=^{16}O$ .<sup>43</sup>

*PVC film; 85 and 10 K; i.r. spectroscopy.* From the preceding sections and from the preliminary report<sup>1</sup> it is obvious that the photochemistry of (1) takes a different course in the gas matrix from the crystalline state. The non-appearance of benzonitrile sulphide, which was expected among the photolysis products in the crystalline samples, could be a consequence of the low quantum yield for conversion of (1) under these circumstances. That self-quenching prevails is also indicated by the fact that no emission is observable from cold, crystalline samples. The benzonitrile sulphide (if formed) is embedded in foreign molecules, *i.e.* the crystal lattice of (1). It maintains full photolytic activity and reacts with high efficiency to produce benzonitrile and sulphur. The overall result is that the steady-state concentration of benzonitrile sulphide in crystalline samples is too small to be observed by i.r. spectroscopy. This situation provoked the idea of employing plastics as media for low-temperature photolysis combined with i.r. spectroscopy. PVC was selected because of its relatively high dissolving power and its transparency between  $1500$  and  $2800\text{ cm}^{-1}$ .

It was possible to cast a PVC film without aggregated molecules ( $1705\text{ cm}^{-1}$ ) in a concentration convenient for i.r. spectroscopy. The monomer absorbs at  $1738\text{ cm}^{-1}$ . Despite the high microscopic viscosity in PVC, the monomeric samples reacted very efficiently to the light (80 K) and photoconversion could be established by irradiation into the very edge of the absorption band at  $470\text{ nm}$ , the wavelength so chosen to minimize secondary photolysis (Figure 11).

The first i.r. bands to be observed after 30 min irradiation at  $470\text{ nm}$  (not shown) were located at  $2330$  ( $CO_2$ ),  $2280$

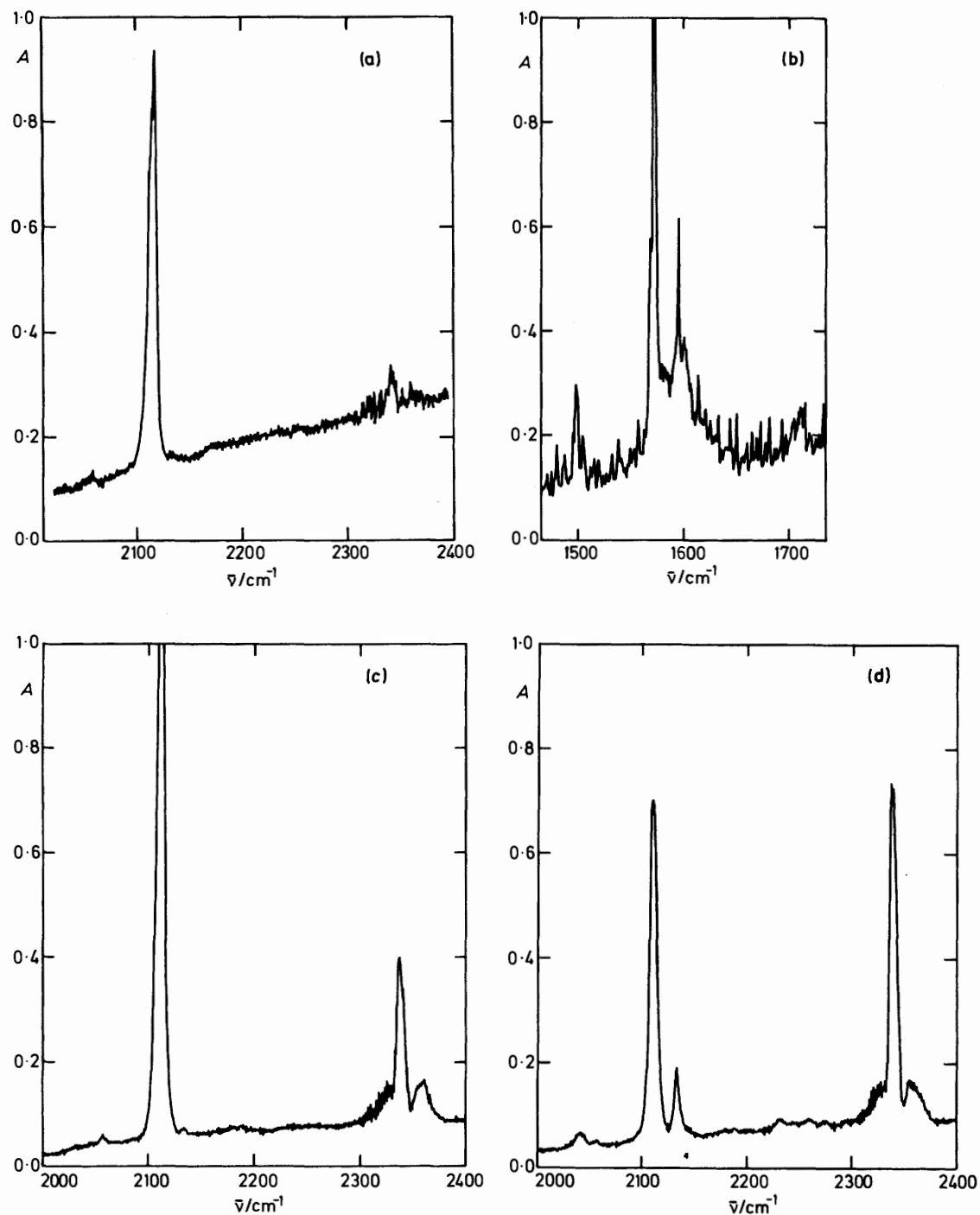


**Figure 8.** I.r. spectra of monomeric (1) in  $N_2$  matrix at 10 K (extinction upwards): (a) heterocumulene region recorded after 20 min irradiation at 431 nm; (b) double-bond region recorded after 32 min irradiation at the same wavelength; (c) heterocumulene region after further 6 min irradiation at 367 nm; (d) further irradiation for 30 min with unscreened light from medium-pressure mercury lamp (Phillips HPK-125)

( $^{13}CO_2$ ; natural occurrence), 2 185 [assigned to benzonitrile sulphide (4)], and 2 100  $cm^{-1}$  [phenyl(nitrosothio)ketene (6)]. Benzonitrile (2 220  $cm^{-1}$ ) appeared after 3.5 h irradiation at this wavelength. The trace labelled (a) in Figure 12 was recorded after exhaustive irradiation at 470 nm and represents maximum intensity achieved by the 2 185  $cm^{-1}$  band. At this point the benzonitrile absorption had become even bigger. Thereafter, the exciting wavelength was changed to 335 nm. After 30 min the 2 185  $cm^{-1}$  band was strongly reduced while a new peak had appeared at 2 030  $cm^{-1}$  [phenyl(oxomethylene)thiyl (7)]. In

Figure 12, trace (b), irradiation at 335 nm had lasted 7.5 h and the band due to (4) at 2 185  $cm^{-1}$  had virtually disappeared. Exposure to Pyrex-filtered light caused reduction in the 2 100  $cm^{-1}$  band and an increase in the 2 030  $cm^{-1}$  band [trace (c)]. This last band proved surprisingly resistant to warm-up, being reduced only 50% at 0 °C and still observable at 50 °C. The last trace disappeared at 60 °C together with  $CO_2$ .

The thermal stability of (4) and (6) was investigated in separate experiments. Both disappeared gradually, the first showing a temperature profile much like the 337 nm absorption

seen by u.v. spectroscopy in PVC. The band at  $2185\text{ cm}^{-1}$  disappeared at  $-60^\circ\text{C}$  while that at  $2100\text{ cm}^{-1}$  was visible until  $10^\circ\text{C}$ .

In sum, benzonitrile sulphide is believed to be responsible for the  $2185\text{ cm}^{-1}$  band for three reasons: (i) it appears before benzonitrile; (ii) it is efficiently photolysed at  $335\text{ nm}$  [where (4) has a maximum]; (iii) it behaves during warm-up in PVC as benzonitrile sulphide does, when monitored by u.v. spectroscopy.

The photolysis ( $489\text{ nm}$ ) of (1) in PVC at  $10\text{ K}$  differed from

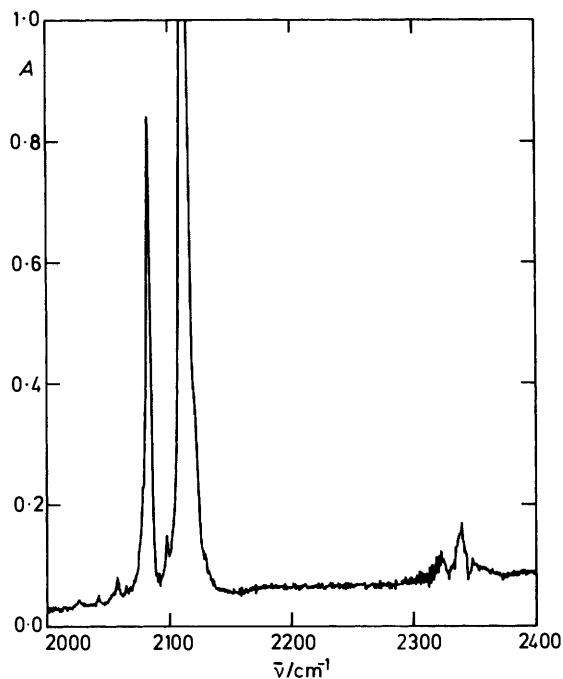


Figure 9. I.r. spectrum (extinction upwards) recorded after 19 min irradiation at  $367\text{ nm}$  of  $^{18}\text{O}$ -labelled (1) embedded as monomers in  $\text{N}_2$  matrix

the experiments at  $85\text{ K}$  in the sense that only  $2330$  ( $^{12}\text{CO}_2$ ),  $2275$  ( $^{13}\text{CO}_2$ ),  $2223$  (benzonitrile), and  $2185\text{ cm}^{-1}$  bands were produced. No absorptions appeared at  $2030\text{ cm}^{-1}$  and only a tiny hump could be seen at  $2105\text{ cm}^{-1}$ .

$\text{N}_2$  Matrix;  $10\text{ K}$ ; u.v. spectroscopy. A sample of (1) on a CsBr disc was prepared at  $20\text{ K}$  under conditions (guest:host ratio)

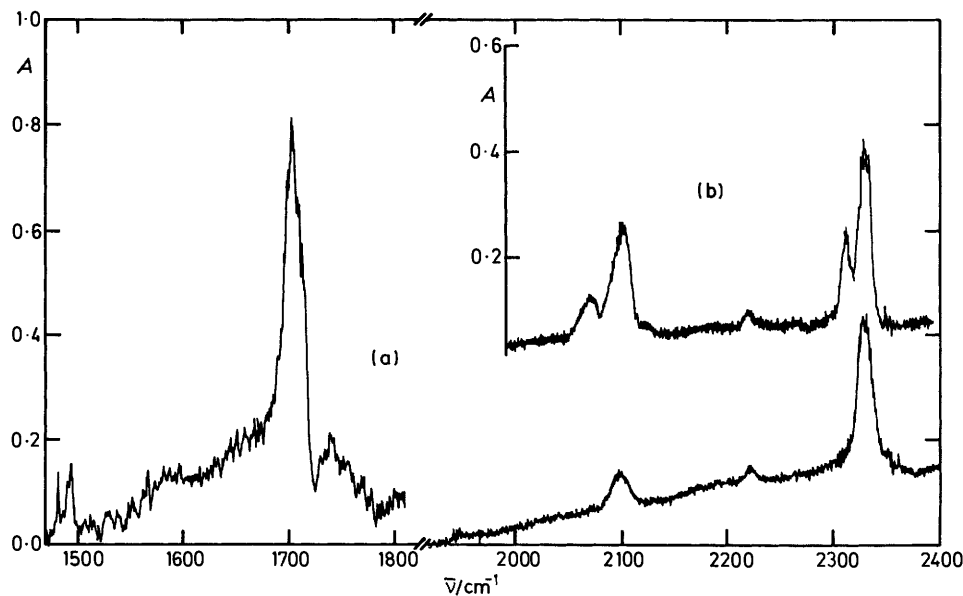
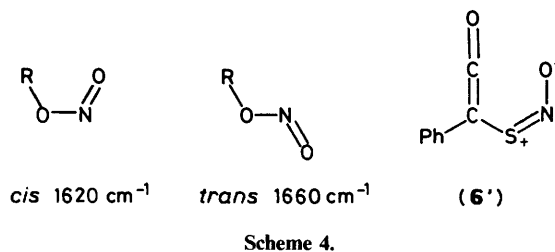
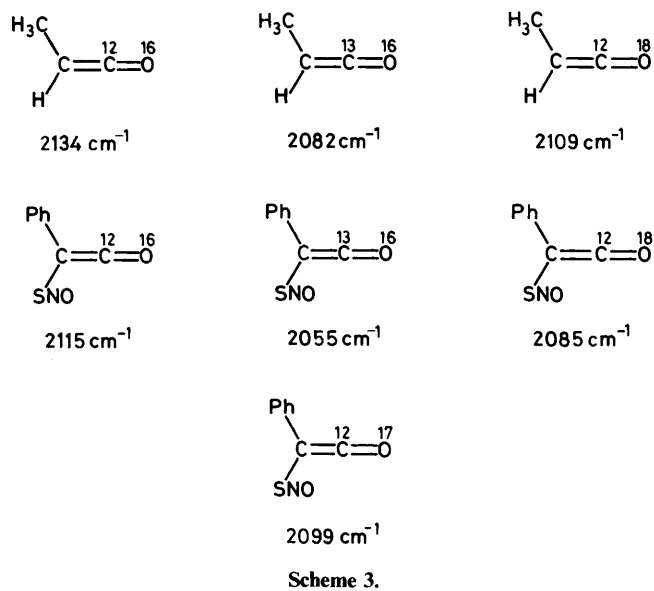
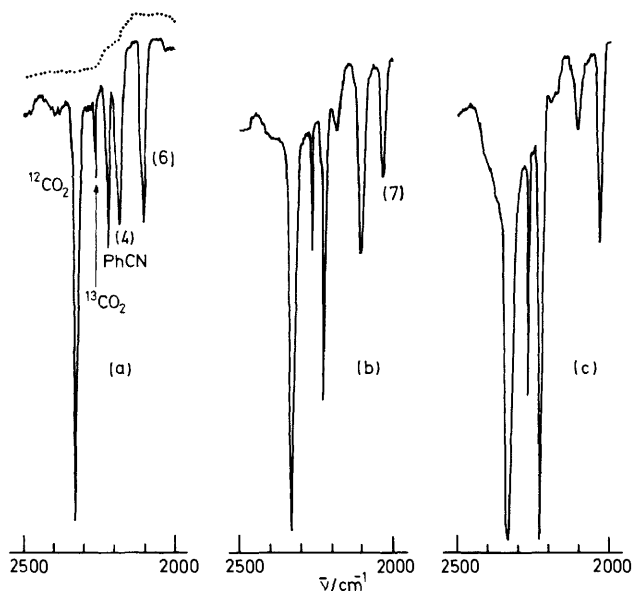
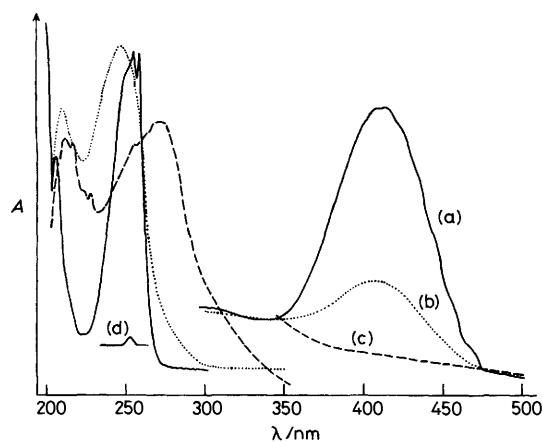


Figure 10. I.r. spectra at  $10\text{ K}$ : (a) recorded after irradiation, at  $367\text{ nm}$  for  $170\text{ min}$ , of a crystal film of (1); (b) recorded after irradiation, at  $367\text{ nm}$  for  $125\text{ min}$ , of a crystal film of  $^{18}\text{O}$ -labelled (30%) (1)





**Figure 11.** I.r. spectra at 85 K (transmission upwards) of (1) in PVC film (0.09 mm): (a) after irradiation for 22 h at  $470 \pm 10$  nm (dotted line: spectrum before photolysis); (b) after further irradiation for 7.5 h at  $335 \pm 10$  nm; (c) after further irradiation for 26 min with Pyrex-filtered light from a high-pressure mercury lamp (Osram HBO-200)



**Figure 12.** U.v. spectra of (1) in  $N_2$  matrix at 10 K: (a) before photolysis; (b) after 4.5 min irradiation at 367 nm (interference filter); (c) after further irradiation for 125 min at 367 nm; (d) background (sloping baselines due to dispersion)

ensuring that minimum aggregation occurred. The resulting spectrum [Figure 12, trace (a)] shows no indications of aggregation (compare Figure 2). The first stages of photolysis proceeded in the same manner whether the excitation was at 448 nm (not shown) or 367 nm [Figure 12, trace (b)]. A substance absorbing at 248 nm was formed. When the sample was subjected twice to annealing (to 30 K) at this stage of photolysis, no spectral changes were observed. Further irradiation with unfiltered light (Philips HPK-125) for a short while (60 s) would cause disappearance of all absorbing material (not shown). Benzonitrile, which is photostable, was not formed. Figure 12 displays three intermediate spectra recorded when 367 nm was used for excitation throughout. Trace (b) represents the maximum concentration of the species absorbing at 248 nm. Gradually it was photolysed to produce a secondary product with a maximum at 272 nm [trace (c)]. No other maxima were observed between 300 and 700 nm. A tiny peak at 229 nm [trace

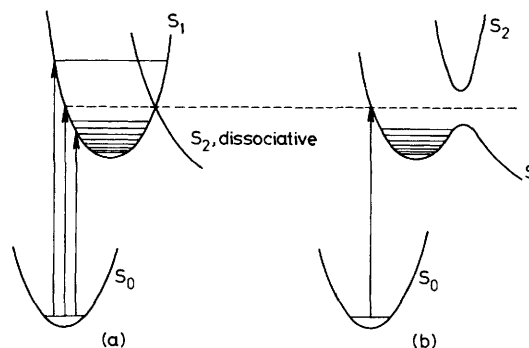


**Figure 13.** Schematic representation of energy potential surfaces for ground and excited singlet states of (1)

(c)] reflects the small amounts of benzonitrile being formed. No spectral changes were observed after annealing of this sample (35 K).

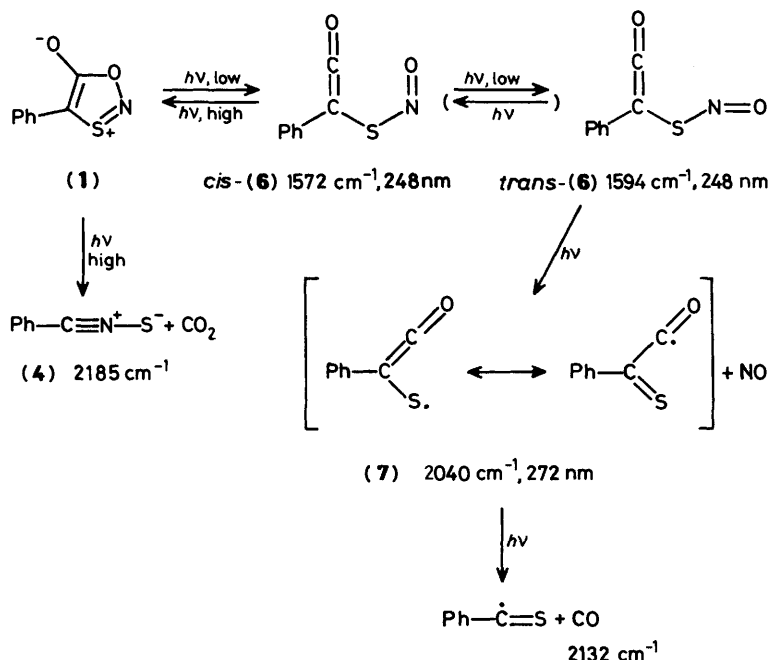
The information obtained by i.r. spectroscopy facilitated interpretation of the u.v. experiments in  $N_2$  matrix at 10 K. As the dominating product, (6) is found absorbing at 248 nm [Figure 8, trace (b)]. When (6) is viewed *a priori* as composed of the chromophores phenylketene and nitrosothiyl it can be expected to display several other weak absorptions at higher wavelengths. Thus phenylmethylketene absorbs at 445 nm ( $\epsilon$  18 l mol<sup>-1</sup> cm<sup>-1</sup>)<sup>44</sup> while *S*-nitrosohexane-1-thiol absorbs at 340 ( $\epsilon$  1 030 l mol<sup>-1</sup> cm<sup>-1</sup>) and at 550 nm ( $\epsilon$  26).<sup>45</sup> As already concluded on the basis of the i.r. frequencies, there must be interference between the different  $\pi$ -systems of (6). Where these electronic transitions are to be located is therefore unpredictable. But they seem too weak to be observable together with the very intense absorption at 248 nm.

This conclusion is supported by the results of continued irradiation at 367 nm, which transforms (6) into (7) (272 nm). Trace (c) also displays a tiny peak at 233 nm, indicating formation of small amounts of benzonitrile. When observed so late in the course of irradiation, this raises the question of photoreversibility of the initial formation of (6).

## Discussion

**Electronic Absorption and Emission Spectroscopy.**—A vibrational fine structure is observed in the long-wavelength absorption band of (1) [ $N_2$  matrix; Figure 12, trace (a)], but it fades and stops on the short-wavelength side of the maximum. This observation tells us something about the excited state surface(s) to which excitation occurs. Figure 13 offers two representations of the situation. The left part shows two upper non-interfering singlet surfaces, one of which ( $S_2$ ) is (pre-)dissociative. To the right, a coupling between the two states is expected, resulting in an avoided crossing;  $S_1$  becomes a dissociative pathway with an activation barrier. Since the molecule (1) has no symmetry elements (the phenyl group is twisted  $16.6^\circ$  out of the plane of the heterocycle),<sup>36</sup> some degree of avoidedness is inevitable. Just how much is reflected in the energy gap between the two states. Qualitatively, Figure 13 displays two extremes and reality must be visualized in between.

The spacing of the vibrational fine structure (400–600 cm<sup>-1</sup>) and the observation of *negative anharmonicity* may be helpful in localizing the vibrational mode involved. Phenyl torsion is usually at much lower frequencies, *i.e.* below 100 cm<sup>-1</sup>.<sup>46</sup> The features do fit out-of-plane bending or so-called pseudorotation of rings, which move in potentials with double minima. The vibrational frequency for a comparable molecule like imidazole is found at 500 cm<sup>-1</sup>.<sup>47</sup> In the ground state, the ring of (1) is planar, with the carbonyl group bent 0.026 Å out of the plane.<sup>36</sup>



Scheme 5.

It is a spectroscopic maxim that the occurrence of a long vibrational progression in an electronic band betrays the vibrational mode responsible for changing the geometry of the initial state into that of the final state. Probably, in the thermally relaxed, electronically excited singlet of (1), the heterocyclic ring is bent.

The concept of two close lying singlet states also explains the discrepancy between the calculated (19 ns) and the measured (65 ns) radiative lifetimes. Dissociative states are not radiative and the area used in the denominator of equation (1) is too large.

There is a slight deviation of the excitation spectrum from the absorption spectrum on the short-wavelength side of the 411 nm band, starting at the wavelength where the vibrational fine structure in the absorption spectrum stops [Figure 1, trace (c)]. Even though the effect is marginal, it may reflect that excitation above the dissociative threshold (Figure 13) implies a smaller quantum yield of fluorescence.

The profile of the quantum yield-temperature dependence (Figure 3) does not fit an Arrhenius plot, but the narrow temperature region in which the fluorescence drops to zero coincides with the temperature (*ca.* 110 K) at which the microscopic viscosity of EPA is known to undergo dramatic changes.<sup>32</sup> Since no fluorescence could be observed from the mesoion in a gas matrix (or crystals) at 10 K but was easily seen in glycerol glasses at 194 K and in polymer film at 194, 77, and 10 K, viscosity and not temperature must be the decisive factor for observation of fluorescence from (1). In the crystalline state self-quenching prevails and damps both photochemistry and fluorescence.

#### Environmental Influence on Photolytic Transformations.—

As seen from the experimental results, local viscosity is a ruling factor in several of the processes involved in the low-temperature photochemistry of (1). *A priori*, higher viscosity is expected to impose restrictions on the nuclear movements and cause raised activation barriers for all processes involving conformational changes leading to a higher molecular volume. Thus associative processes are favoured over dissociative processes. Owing to opposite signs for the activation entropy, lowering the temperature helps in the same direction. Scheme 5

sums up the (photo)chemical processes involved in the low-temperature photochemistry of (1). The terms 'high' and 'low' indicate viscosities favouring the indicated conversion *relative* to competing processes.

Among the primary photoprocesses, ring-opening of (1) to *cis*-(6) prevails over elimination of carbon dioxide in a soft medium like a gas matrix. Elimination is possible but relatively slow. In harder media like EPA or PVC, or in the crystalline or aggregated states, elimination competes efficiently with ring-opening. While (6) is formed along with (4) in PVC at 85 K (Figure 11), virtually no ketene is observed upon irradiation of (1) at 10 K. Since the wavelength chosen for photolysis (489 nm) was inefficient for reversing the conversion of (6) into (1) (see later), it must be concluded that ring-opening is completely suppressed under these circumstances.

In agreement with the principle of least motion, *cis*-(6) (1 572  $\text{cm}^{-1}$ ) was observed first in  $\text{N}_2$  matrix while *trans*-(6) (1 594  $\text{cm}^{-1}$ ) was a result of prolonged irradiation. In Scheme 5 the two structures are connected with a reaction arrow. Among them, only *cis*-(6) can perform a symmetry-allowed [2 + 2] photocycloaddition which will regenerate [formally *via* (2)] the starting material. A rigid matrix can keep the atoms in their original positions and make re-formation of (1) compete with *cis-trans* isomerization and homolysis of the S-N bond of *cis*-(6). This may be why the preparative photolysis, at 77 K, of a  $10^{-2}\text{M}$ -solution of (1) in ethanol left 70% benzonitrile to be detected by g.l.c. after thawing. This figure has to be compared with the 21% (aerated), 49% (argon purged), and 100% (under NO) obtained after photolysis at room temperature in the same medium.<sup>15</sup> Further indication of reversibility is found in the EPA experiments [Figure 6, traces (b) and (c)]. Initially, 95% starting material was photolysed by monochromatic irradiation into the main absorption band of (1). Thereafter, the exciting wavelength was shifted 45 nm towards the u.v. The outcome was a surprising increase of more than 50% in the yield of benzonitrile sulphide. Something is formed along with benzonitrile sulphide from the excited state of (1). This species can produce more (4) on irradiation at 370 nm either in a direct photochemical process or *via* re-formation of starting material. The first possibility involves participation of a new, photo-

chemical precursor of benzonitrile sulphide. This must be formed *in parallel* with the benzonitrile sulphide observed after the irradiation at 415 nm [Figure 6, trace (b)], otherwise the transformation would not display isosbestic points (Figure 4). It is illogical that (1) should be able to produce (4) and another molecule, which also can form (4) in a subsequent photolytic step. Furthermore, none of the other experiments, in particular the low-temperature i.r. experiments in PVC, has shown indications of such a species. Consequently, the observations are most easily explained by a photochemical back-reaction of (6) to (1). Apparently (6) has a weak absorption in the 350 nm region, which is not revealed as a maximum in Figure 12, trace (b). The reversibility is also reflected in the fact that the extinction coefficient calculated from the spectra (a) and (c) in Figure 6 for benzonitrile sulphide is twice as large as the value derived from the initial slopes of the traces in Figure 5. Furthermore, the straight-line deviations of Figure 5 start earlier and get bigger the larger the initial concentration of mesoion. Thus, (6) is pumped back to (1), which then is rephotolysed to benzonitrile sulphide and carbon dioxide. By choosing the proper circumstances, elimination can be maximized, a situation we believe is established in Figure 6, trace (c).

Photoreversibility of (6) to (1) *does occur* in N<sub>2</sub> matrices, but with a much smaller quantum yield. After complete conversion of starting material, extended irradiation produces carbon dioxide [i.r. absorption, Figure 8, traces (c) and (d)] and benzonitrile [u.v. absorption, Figure 12, trace (c)] in increasing but still very small amounts (both molecules absorb strongly under the circumstances).

Likewise, the qualitative nature of these considerations is also reflected in the fact that homolytic cleavage of (6) to (7) does occur in PVC at 85 K. Extended irradiation of the highly concentrated i.r. sample produces the 2 040 cm<sup>-1</sup> band of (7) [Figure 11, trace (c)].

One structure notable for its absence throughout the i.r. study is (2). As mentioned at the outset, this valence tautomer is used to rationalize the primary reactions whenever a mesoion is found to undergo elimination of a heterocumulene. If present, (2) would have been easily observable, absorbing in the neighbourhood of fused β-lactams at 1 770–1 780 cm<sup>-1</sup>.<sup>48</sup> The structure of (2) does not show any features indicating an extreme thermal instability. Therefore the question arises as to whether bicyclic valence isomers ought to be the first choice as the primary photoproduct of mesoions.<sup>20–23</sup>

Similarly, no i.r. absorption which can be ascribed to the presence of phenylthiazirine (3) has been located. Since its absorption frequency may be harder to predict, this species could have been masked by the strong absorptions of PVC. Alternatively, the high concentrations employed in i.r. spectroscopy may have encouraged rephotolysis or the temperature may still have been too high to stabilize this precursor of benzonitrile sulphide. In any case, the intermediacy of (3) remains an open question.

**Potential Surfaces.**—Since the photochemistry of (1) follows a singlet pathway, it is possible to bring the results from the electron spectroscopy and the low-temperature photolysis together, *i.e.* we can extend the potential-energy surfaces in Figure 13 to serve as a basis for rationalizing the photochemistry (Figure 14).

Since rigid media, other things being equal, must be expected to suppress dissociative reactions over associative, and formation of (6) proceeds with high quantum yields in the soft N<sub>2</sub> matrix, we assign this reaction to the pathway along the dissociative part of the singlet surface (Figure 14). Fluorescence from the monomeric molecules was observed in rigid media only. Under the same circumstances formation of (6) was retarded relative to elimination. In the light of coincidence,

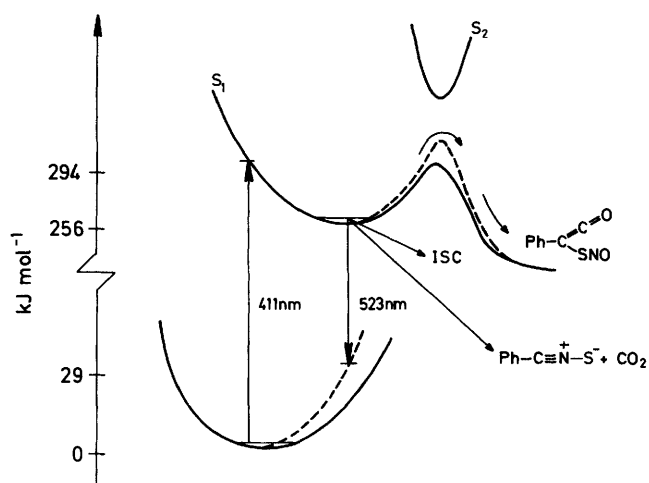
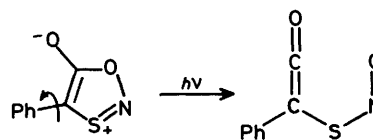


Figure 14. Potential-energy surfaces for ground and excited singlet states of (1) showing reaction barriers being influenced by high viscosity (broken lines). Fixed points on the energy scale are derived from the spectra in Figure 1



Scheme 6.

formation of (6) looks like *the* reaction deactivating the relaxed singlet manifold efficiently in soft surroundings. When strain is put on nuclear motion, this energy drain is blocked and the singlet excited molecule is forced to emit at 523 nm, undergo elimination of carbon dioxide, or cross over to a non-reacting and non-phosphorescing triplet.

At the beginning of this paper, several examples were presented of systems showing viscosity-sensitive fluorescence. In a majority of cases phenyl torsion has been identified as the critical deactivation mode sensitive to environmental factors. A similar mechanism may be operating in our case. In the ground state, the phenyl group of (1) is twisted 16.6° out of the plane of the heterocycle.<sup>36</sup> The reaction from the Franck-Condon excited state of (1) to (6) may require a twist of the phenyl group in order for its π-system to line up with that of the heterocycle (Scheme 6). Preventing this may very well be the primary mode of action of a rigid environment, thus blocking the formation of (6).

#### Acknowledgements

We thank Dr. M. Chow and Professor N. Turro, Columbia University, New York, for the single-photon counting determination of the emission lifetime. The gas matrix experiments were performed at the University of Newcastle upon Tyne. We also thank Dr. R. N. Perutz for his help. The low-temperature u.v. cell used in Copenhagen was constructed by Dr. S. Harnung of the Inorganic Chemistry Department. The Danish Natural Science Research Council is acknowledged for financial support, for purchase of the emission spectrophotometer, and for supporting the work in Newcastle with a travel grant.

#### References

- I. R. Dunkin, M. Poliakoff, J. J. Turner, N. Harrit, and A. Holm, *Tetrahedron Lett.*, 1976, 873.
- P. J. Wagner, M. May, and A. Haug, *Chem. Phys. Lett.*, 1972, 13, 545.

- 3 G. C. Schmidt, *Wied. Ann.*, 1896, **58**, 103; G. C. Schmidt, *Ann. Physik*, 1921, **65**, 247; G. Oster, *C.R. Acad. Sci.*, 1951, **232**, 1708; G. Oster and Y. Nishijima, *J. Am. Chem. Soc.*, 1956, **78**, 1581; G. Oster, J. Jousset-Dubien, and B. Brody, *ibid.*, 1959, **81**, 1869; T. Förster and G. Hoffmann, *Z. Phys. Chem. (Frankfurt)*, 1971, **75**, 63; W. Yu, F. Pellegrino, M. Grant, and R. R. Alfano, *J. Chem. Phys.*, 1977, **67**, 1766; L. A. Brey, G. B. Schuster, and H. G. Drickamer, *ibid.*, p. 2648; D. Magde and M. W. Windsor, *Chem. Phys. Lett.*, 1974, **24**, 144; M. D. Hirsch and H. Mahr, *ibid.*, 1979, **60**, 299; E. P. Ippen, C. V. Shank, and A. Bergman, *ibid.*, 1976, **38**, 611; P. Wirth, S. Schneider, and F. Dörr, *Opt. Commun.*, 1977, **20**, 155; C. J. Mastrangelo and H. W. Offen, *Chem. Phys. Lett.*, 1977, **46**, 588.
- 4 S. Sharafy and K. A. Muszkat, *J. Am. Chem. Soc.*, 1971, **93**, 4119; D. Gegiou, K. A. Muszkat, and E. Fischer, *ibid.*, 1968, **90**, 12; G. Fischer, G. Seger, K. A. Muszkat, and E. Fischer, *J. Chem. Soc., Perkin Trans. 2*, 1975, 1569; L. A. Brey, G. B. Schuster, and H. G. Drickamer, *J. Am. Chem. Soc.*, 1979, **101**, 129.
- 5 M. Belletete and G. Durocher, *Can. J. Spectrosc.*, 1979, **24**, 87.
- 6 T. Bercovici, R. Korenstein, K. A. Muszkat, and E. Fischer, *Pure Appl. Chem.*, 1970, **24**, 531.
- 7 J. Kordas and M. A. El-Bayoumi, *J. Am. Chem. Soc.*, 1974, **96**, 3043.
- 8 H.-D. Becker, K. Sandros, and L. Hansen, *J. Org. Chem.*, 1981, **46**, 821.
- 9 K. Y. Law, *Chem. Phys. Lett.*, 1980, **75**, 545; R. O. Loutfy, *Macromolecules*, 1981, **14**, 270; R. O. Loutfy and B. A. Arnold, *J. Phys. Chem.*, 1982, **86**, 4205; K. Y. Law and R. O. Loutfy, *Macromolecules*, 1981, **14**, 587.
- 10 A. T. Eske and K. R. Naqui, *Chem. Phys. Lett.*, 1979, **63**, 128; J. Jaraudias, *J. Photochem.*, 1980, **13**, 35; E. Blatt, F. E. Treolar, K. P. Ghigginio, and R. G. Gilbert, *J. Phys. Chem.*, 1981, **85**, 2810; K. R. Naqui, J. Donatsch, and U. P. Wild, *Chem. Phys. Lett.*, 1975, **34**, 285; K. A. Al-Hassan and M. A. El-Bayoumi, *ibid.*, 1980, **76**, 121.
- 11 G. Smets, *Pure Appl. Chem.*, 1972, **30**, 1; 1975, **42**, 509; G. Smets and S. Matsumoto, *J. Polym. Sci.*, 1976, **14**, 2983.
- 12 T. Matsumoto, M. Sato, and S. Hirayama, *Chem. Phys. Lett.*, 1972, **13**, 13; 1973, **18**, 563.
- 13 T. Matsumoto, M. Sato, and S. Hirayama, *Chem. Phys. Lett.*, 1974, **27**, 237.
- 14 T. Bacchetti and A. Alemagna, *Atti Accad. Nazl. Lincei, Rend. Classe Sci. Fis., Mat. Nat.*, 1960, **23**, 646 (*Chem. Abstr.*, 1961, **55**, 9382); H. Gotthardt, *Tetrahedron Lett.*, 1971, 1277; H. Gotthardt, *Chem. Ber.*, 1972, **105**, 188.
- 15 A. Holm, N. Harrit, and N. H. Toubro, *Tetrahedron*, 1976, **32**, 2559.
- 16 H. Gotthardt, F. Reiter, and C. Kromer, *Liebigs Ann. Chem.*, 1981, 1025.
- 17 A. Holm, N. Harrit, K. Bechgaard, O. Buchardt, and S. E. Harnung, *J. Chem. Soc., Chem. Commun.*, 1972, 1125.
- 18 A. Holm, N. Harrit, and I. Trabjerg, *J. Chem. Soc., Perkin Trans. 1*, 1978, 746.
- 19 J. C. Earl and A. W. Mackney, *J. Chem. Soc.*, 1935, 899.
- 20 H.-J. Piek, Dissertation, Bonn, 1968; C. H. Krauch, J. Kuhls, and H.-J. Piek, *Tetrahedron Lett.*, 1966, 4043.
- 21 C. S. Angadiyavar and M. V. George, *J. Org. Chem.*, 1971, **36**, 1589; A. Chinone, Y. Huseya, and M. Ohta, *Bull. Chem. Soc. Jpn.*, 1970, **43**, 2650; H. Gotthardt and F. Reiter, *Tetrahedron Lett.*, 1971, 2749; Y. Huseya, A. Chinone, and M. Ohta, *Bull. Chem. Soc. Jpn.*, 1971, **44**, 1667; 1972, **45**, 3202; M. Märky, H.-J. Hansen, and H. Schmid, *Helv. Chim. Acta*, 1971, **54**, 1275.
- 22 G. Eber, S. Schneider, and F. Dörr, *Ber. Bunsenges. Phys. Chem.*, 1980, **84**, 281.
- 23 H. Kato, T. Shiba, H. Yoshida, and S. Fujimori, *Chem. Commun.*, 1970, 1591; H. Kato, M. Kawamura, and T. Shiba, *ibid.*, p. 959.
- 24 R. M. Moriarty, R. Mukherjee, O. L. Chapman, and D. R. Eckroth, *Tetrahedron Lett.*, 1971, 397; A. Holm, N. H. Toubro, and N. Harrit, *ibid.*, 1976, 1909.
- 25 T. R. Evans, *J. Photochem.*, 1982, **19**, 55.
- 26 C. L. Pedersen, N. Harrit, M. Poliakoff, and I. Dunkin, *Acta Chem. Scand., Ser. B*, 1977, **31**, 848.
- 27 C. A. Parker and C. G. Hatchard, *Analyst (London)*, 1962, **87**, 664.
- 28 N. J. Turro and G. L. Farrington, *J. Am. Chem. Soc.*, 1980, **102**, 6051.
- 29 K. B. Wiberg and A. S. Fox, *J. Am. Chem. Soc.*, 1963, **85**, 3487.
- 30 J. Sauer and C. Jung, *Z. Phys. Chem. (Leipzig)*, 1974, **255**, 412.
- 31 N. J. Turro, 'Molecular Photochemistry,' Benjamin, New York, 1967, p. 48.
- 32 A. Martinez and D. Dornic, *J. Chim. Phys.*, 1969, **66**, 817.
- 33 C. A. Parker, 'Photoluminescence of Solutions,' Elsevier, Amsterdam, (a) p. 247; (b) p. 262; (c) p. 208.
- 34 L. Doub and J. M. Vandenberg, *J. Am. Chem. Soc.*, 1947, **69**, 2714.
- 35 B. Saville, *Analyst (London)*, 1958, **83**, 670.
- 36 G. D. Andretti, G. Bocelli, L. Cavalca, and P. Sgarabotto, *Gazz. Chim. Ital.*, 1972, **102**, 23.
- 37 G. E. Leroi, G. E. Ewing, and G. C. Pimentel, *J. Chem. Phys.*, 1964, **40**, 2298.
- 38 F. Nicolaisen, the H. C. Ørsted Institute, personal communication.
- 39 L. J. Bellamy, 'Advances in Infrared Group Frequencies,' Methuen, London, 1968.
- 40 R. J. Philippe and H. Moore, *Spectrochim. Acta*, 1961, **17**, 1004.
- 41 R. J. Philippe, *J. Mol. Spectrosc.*, 1961, **6**, 492.
- 42 G. Kresze and U. Uhlich, *Chem. Ber.*, 1959, **92**, 1048.
- 43 L. Fredin, B. Nelander, and G. Ribbegaard, *J. Mol. Spectrosc.*, 1974, **53**, 410.
- 44 H. Pracejus and J. Leska, *Z. Naturforsch., Teil B*, 1966, **21**, 30.
- 45 J. Barrett, L. J. Fritzgibbons, J. Glauser, R. H. Still, and P. N. W. Young, *Nature (London)*, 1966, **211**, 848.
- 46 L. A. Carreira and T. G. Towns, *J. Mol. Struct.*, 1977, **41**, 1; H. Takeuchi, S. Suzuki, A. J. Dianoux, and G. Allen, *Chem. Phys.*, 1981, **55**, 153.
- 47 P. G. Lister, J. N. MacDonald, and N. L. Owen, 'Internal Rotation and Inversion,' Academic Press, London, 1978, pp. 208, 219.
- 48 N. B. Colthup, L. H. Daly, and S. E. Wiberley, 'Introduction to Infrared and Raman Spectroscopy,' Academic Press, New York, 1964, p. 265.

Received 14th July 1986; Paper 6/1394